

INTEGRATING EEG AND MEG SIGNALS TO IMPROVE MOTOR IMAGERY CLASSIFICATION IN BRAIN-COMPUTER INTERFACE

MARIE-CONSTANCE CORSI

Inria Paris, Aramis project-team, 75013, Paris, France
Sorbonne Universités, UPMC Univ Paris 06, Inserm, CNRS, Institut du cerveau et la moelle (ICM) - Hôpital
Pitié-Salpêtrière,
Boulevard de l'hôpital, F-75013, Paris, France

MARIO CHAVEZ

CNRS UMR7225, Hôpital Pitié-Salpêtrière, Paris, France

DENIS SCHWARTZ, LAURENT HUGUEVILLE

Centre de NeuroImagerie de Recherche - CENIR,
Centre de Recherche de l'Institut du Cerveau et de la Moelle Epinière,
Université Pierre et Marie Curie-Paris 6 UMR-S975, Inserm U975, CNRS UMR7225, Groupe Hospitalier
Pitié-Salpêtrière, Paris, France

ANKIT N. KHAMBHATI

Department of Bioengineering, University of Pennsylvania, Philadelphia, PA, 19104, USA

DANIELLE S. BASSETT

Department of Bioengineering, University of Pennsylvania, Philadelphia, PA, 19104, USA
Department of Electrical and Systems Engineering, University of Pennsylvania, Philadelphia, PA, 19104, USA
Department of Physics, University of Pennsylvania, Philadelphia, PA, 19104, USA
Department of Neurology, University of Pennsylvania, Philadelphia, PA, 19104, USA

FABRIZIO DE VICO FALLANI

Inria Paris, Aramis project-team, 75013, Paris, France
Sorbonne Universités, UPMC Univ Paris 06, Inserm, CNRS, Institut du cerveau et la moelle (ICM) - Hôpital
Pitié-Salpêtrière,
Boulevard de l'hôpital, F-75013, Paris, France
E-mail: fabrizio.devicofallani@gmail.com

We adopted a fusion approach that combines features from simultaneously recorded electroencephalographic (EEG) and magnetoencephalographic (MEG) signals to improve classification performances in motor imagery-based brain-computer interfaces (BCIs). We applied our approach to a group of 15 healthy subjects and found a significant classification performance enhancement as compared to standard single-modality approaches in the alpha and beta bands. Taken together, our findings demonstrate the advantage of considering multimodal approaches as complementary tools for improving the impact of non-invasive BCIs.

Keywords: classifier fusion; EEG; MEG; brain-computer interface; motor imagery.

1. Introduction

Brain-computer interfaces (BCIs) exploit the ability of subjects to modulate their brain activity through intentional mental effort, such as in motor imagery (MI). BCIs are increasingly used for control and communication,^{1–11} and for the treatment of neurological disorders.^{12–17}

Despite their societal and clinical impact, many engineering challenges remain, from the optimization of the control features to the identification of the best mental strategy to code the user's intent.¹⁸ Furthermore, between 15 and 30 % of the users are affected by a phenomenon called “BCI illiteracy”¹⁹ which consists in not being able to control properly a BCI even after several training sessions. BCI illiteracy particularly concerns MI-based BCIs because of the inherent difficulty to produce distinguishable brain activity patterns.²⁰

These challenges critically affect the usability of MI-based BCIs²¹ and have motivated, on the one hand, a deeper understanding of mechanisms associated with MI,^{22–25} and on the other hand the research of new features to enhance BCI performance for both healthy subjects and patients.^{26–29} In the latter case, hybrid and multimodal approaches adding respectively different type of biosignals^{27,30} and neuroimaging data, such as near-infrared spectroscopy (NIRS)^{31–34} and functional magnetic resonance imaging (fMRI),³⁵ have been proven to increase the overall performance.

Here, we consider magnetoencephalography (MEG), which carries complementary information in terms of source depth³⁶ and conductivity^{37–40} sensitivities, but also radially/tangentially oriented dipole detection.^{41,42,43} While previous studies have demonstrated the feasibility of BCI⁴⁴ and neurofeedback,⁴⁵ based on MEG activity, the potential benefit of the combination with EEG signals has been poorly explored. Indeed, such integration might have practical consequences in the light of the recent development of portable MEG sensors, based on optically pumped magnetometers.⁴³

To address this gap in knowledge, we considered high-density EEG and MEG signals simultaneously recorded in a group of healthy subjects during a MI-based BCI task. We then propose a matching-score fusion approach to test the ability to improve the classification of motor-imagery associated with BCI

performance.

2. Materials and Methods

2.1. *Simultaneous E/MEG recordings*

Fifteen healthy subjects (aged 28.13 ± 4.10 years, 7 women), all right-handed, participated in the study. None presented with medical or psychological disorders. According to the declaration of Helsinki, written informed consent was obtained from subjects after explanation of the study, which was approved by the ethical committee CPP-IDF-VI of Paris. All participants received financial compensation at the end of their participation. MEG and EEG data were simultaneously recorded with, respectively, an Elekta Neuromag TRIUX[®] machine (which includes 204 planar gradiometers and 102 magnetometers) and with a 74 EEG-channel system. The EEG electrodes positions on the scalp followed the standard 10-10 montage. EEG signals were referenced to mastoid signals, with the ground electrode located at the left scapula, and impedances were kept lower than 20 kOhms. On average, 1.5 hours was needed for subjects preparation (i.e. explaining the protocol, placing the electrodes, registering the EEG sensor positions and checking the impedances). M/EEG data were recorded in a magnetically shielded room with a sampling frequency of 1 kHz and a bandwidth of 0.01-300 Hz. The subjects were seated in front of a screen at a distance of 90 cm. To ensure the stability of the position of the hands, the subjects laid their arms on a comfortable support, with palms facing upward. We also recorded electromyogram (EMG) signals from the left and right arm of subjects. Expert bioengineers visually inspected EMG activity to ensure that subjects were not moving their forearms during the recording sessions. We carried out BCI sessions with EEG signals transmitted to the BCI2000 toolbox⁴⁶ via the Fieldtrip buffer.⁴⁷

2.2. *BCI protocol*

We used the one-dimensional, two-target, right-justified box task,⁴⁸ where subjects had to perform a sustained MI (grasping) of the right hand to hit up-targets, while remaining at rest to hit down-targets. Each run consisted of 32 trials with up and down targets, consisting of a grey vertical bar displayed on the right portion of the screen, equally and randomly distributed across trials.

The experiment was divided into two phases:

- (i) **Training:** The training phase consisted of five consecutive runs without any feedback. For a given trial, the first second corresponded to the inter-stimulus interval (ISI), where a black screen was presented to the subject. The target appeared and persisted on the screen during subsequent five seconds (from 1 s to 6 s). During this period subjects had to perform the instructed mental tasks.
- (ii) **Testing:** The testing phase consisted of six runs with a visual feedback. For a given trial, the first second corresponded to the ISI, while the target was presented throughout the subsequent five seconds, with the same modalities just as in the training phase. In the last three seconds (from 3 s to 6 s), subjects received a visual feedback to control an object that consists of a cursor (a ball here) that starts from the left-middle part of the screen and moves to the right part of the screen with fixed velocity. This gave a fixed rate of communication of 20 commands/minute. Only vertical position was controlled by the subject’s brain activity and it was updated every 28 ms. The aim is to hit the target with the ball according to the instructed mental tasks, i.e. MI for up-targets; resting for down-targets.

2.3. Signal processing and features extraction

We considered both EEG and MEG activity, the latter consisting of magnetometer (MAG) and gradiometer (GRAD) signals which, given their physical properties, can be processed separately.⁴⁹

As a preliminary step, temporal Signal Space Separation (tSSS)⁵⁰ was performed using MaxFilter (Elekta Neuromag) to remove environmental noise from MEG activity. All signals were downsampled to 250 Hz and segmented into epochs of five seconds corresponding to the target period. To simulate online scenarios, no artifact removal method was applied. Expert bioengineers visually inspected the recorded traces to ensure that no major artifacts (e.g. MEG jumps, EEG pops) were present. After verification, we then kept all the available epochs.

We computed for each sensor the power spectrum between 4 and 40 Hz, with a 1 Hz frequency bin resolution, for both MI and rest epochs. To this

end, we used a multi-taper frequency transformation based on discrete prolate spheroidal sequences (Slepian sequences⁵¹) considered as tapers through the use of the Fieldtrip toolbox.⁴⁷ A ± 0.5 Hz spectral smoothing through multi-tapering was applied.

At this stage, each epoch was characterized by a feature matrix \mathbf{M}_i , containing the power spectrum values for every couple of sensor and frequency bin, and whose dimension was 74×36 , 102×36 and 204×36 , respectively for $i = EEG, MAG, GRAD$.

We adopted a semi-automatic procedure to extract the most relevant features from the matrices \mathbf{M}_i in the training phase. First, we focused on sensors in the motor area contralateral to the movement (see Appendix A.1). In this way, the size of the feature matrices became 8×36 , 11×36 and 22×36 respectively for EEG, MAG, and GRAD. Second, for each selected sensor and frequency bin, we performed a non-parametric cluster-based permutation t-test between the power spectrum values of the MI and rest epochs.^{2,52} To this end, we set a statistical threshold of $p < 0.05$, false-discovery rate corrected for multiple comparisons, and 500 permutations.

We finally extracted the N_f most discriminant features within the standard frequency bands $b = theta$ (4–7 Hz), $alpha$ (8–13 Hz), $beta$ (14–29 Hz), $gamma$ (30–40 Hz). This allowed us to identify, for each modality i and band b , the best (sensor, frequency bin) couples to be used in the testing phase to compute the features \hat{m} . Hence, the final feature vectors used for the classification are given by:

$$\zeta_{i,b} = [\hat{m}_{i,b}^1, \dots, \hat{m}_{i,b}^{N_f}], \quad (1)$$

where $N_f = 1 \dots, 10$. The maximal limit of 10 was chosen based on the actual number of features (between 4 and 6) that we used in the recording sessions, conforming to the guidelines associated with similar MI-based BCI and EEG montages.⁴⁶

2.4. Classification, fusion, and performance evaluation

We performed a separate classification for each value of N_f . Given the relatively small number of features, we used a five-fold cross-validation in a linear discriminant analysis-based (LDA) classification.^{53,54} LDAs are particularly suited for two-class MI-based BCIs.⁵⁵

To integrate the information from different modalities we used a Bayesian fusion approach based on the weighted average method.^{56–58} Similar to what has been proposed for hybrid-BCI systems,³⁰ we linearly combined the posterior probabilities p_i , obtained from the classification of each modality i , weighted by the parameter λ_i :

$$\lambda_i = \frac{p_i}{p_{EEG} + p_{MAG} + p_{GRAD}}. \quad (2)$$

In this manner, a higher weight was assigned to the modality that best classified the data (see Figure 1).

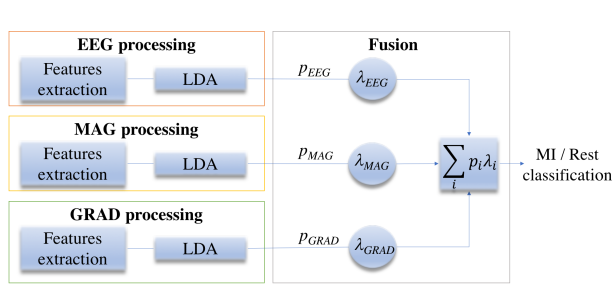


Figure 1. Classifier fusion approach for a given frequency bin. The variables p_i and λ_i stand for the posterior probability and the weight parameter associated with the modality i , respectively.

To assess the classifier performance, we measured the area under the receiver operating characteristic (ROC) curve (AUC) of the computed values of the false positive rate versus the true positive rate. AUC values typically range between one-half (chance level) and one (perfect classification).⁵⁹ We evaluated our fusion approach with respect to the results obtained in each single modality separately (EEG, MAG, GRAD). In addition, we tested the effect of including an increasing number of most significant features.

To statistically compare the results, we input the corresponding AUC values into a nonparametric permutation-based ANOVA with two factors: modality (EEG, MAG, GRAD, Fusion) and features ($N_f = 1, 2, \dots, 10$). A statistical threshold of $p < 0.05$ and 5000 permutations were fixed. We finally used a Tukey-Kramer method⁶⁰ to perform a post-hoc analysis with a statistical threshold of $p < 0.05$. This analysis was performed using routines available in the standard MATLAB and the EEGLAB toolboxes.⁶¹

3. Results

Figure 2 shows the grand-average time-frequency maps of the event-related de/synchronization (ERD/S) computed from the MI trials in the testing phase:⁶² $ERD/S = 100 \times \frac{x_{target} - \mu_{base}}{\mu_{base}}$ where x_{target} was the time-frequency energy of a sensor’s signal for the target period (1–6)s and μ_{base} was the corresponding time-averaged energy in the baseline (0–1)s.

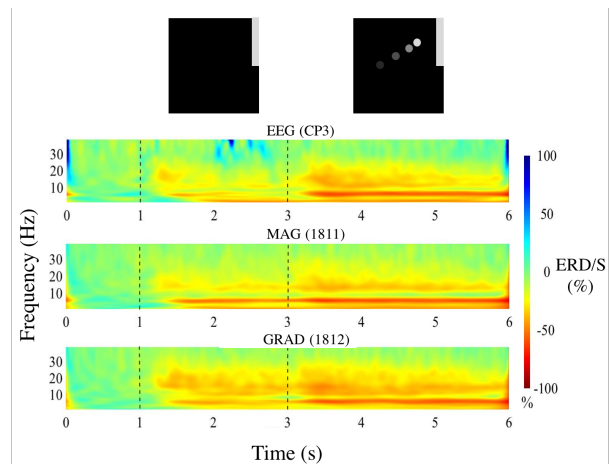


Figure 2. Grand-average time-frequency maps of ERD/S. Top panels illustrate the visual stimulus that appeared during the target period. Dashed lines mark the start of the target presentation and the feedback periods (see section 2.2, testing phase). The time-frequency decomposition of the signals was obtained through Morlet wavelets between 4 and 40 Hz, with a central frequency of 1 Hz associated with a time resolution of 3 s via the Brainstorm toolbox.⁶³ Positive ERD/S values indicate percentage increases (i.e. neural activity synchronization), while negative values stand for percentage decreases (i.e. neural activity desynchronization)

In all modalities, we observed significant changes for the alpha (ERD $\simeq -100\%$) and beta band (ERD $\simeq -60\%$).^{64–66} ERDs started to appear just after the target appearance ($t = 1$ s) and became stronger during the feedback period ($t = 3$ –6 s). Notably, ERDs tended to appear early in the MEG signals as compared to the EEG signals.

Figure 3 illustrates the candidate features that were selected through the semi-automatic procedure for each modality in the training phase. Features ob-

tained from MEG signals tended to be more focused both in space (around the primary motor areas of the hand) and in frequency (mostly in the alpha band). This finding was in line with the fact that lower ERDs were observed in the beta band (see Figure 2).

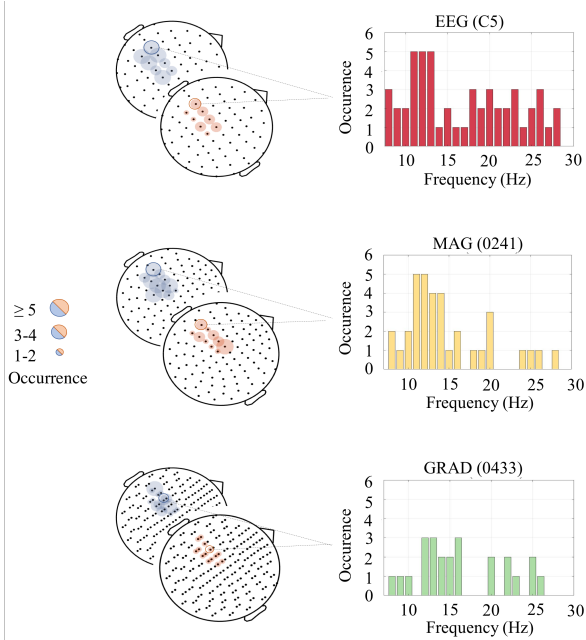


Figure 3. Spatial and frequency distribution of the features selected for classification in each modality. On the left side, the color of the nodes identifies the frequency band (blue for alpha band and red for beta band). The size of the circles is proportional to the number of subjects exhibiting that specific sensor as the best feature. On the right, the histograms detail the occurrences in every frequency bin for the sensor that was most frequently selected.

Fusion improves classification performance

In all frequency bands, the type of modality significantly affected the AUC values (ANOVA, $p < 10^{-3}$), whereas the number of features did not have a significant impact ($p > 0.05$). The AUC values obtained with the fusion approach were significantly higher than those obtained with any other modality (Tukey-Kramer post-hoc, $p < 0.016$), ex-

cept for theta and gamma bands for which we did not observe significant improvements with respect to EEG. The highest classification performance was obtained in the alpha band (Figure 4), for which we also reported here a significant interaction effect between modality and number of features (ANOVA, $p = 0.0069$). In this case, the AUC values with the fusion were significantly higher than those obtained with EEG, MAG, or GRAD separately (Tukey-Kramer post-hoc, $p = 4.3 \times 10^{-9}$, 3.9×10^{-7} , and 0.012).

To evaluate the classification performance in every subject, we considered for each modality the optimal number of features N_f and the best frequency band associated with the highest AUC. Results showed that in thirteen subjects, the fusion led to a better performance as compared to single modalities, with AUC values ranging from 0.55 to 0.85, and relative increments ranging from 1.3% to 50.9% (with an average of $12.8 \pm 6\%$). In only three subjects, the fusion gave equivalent performance (see Table 1). More specifically, if we compared the performances obtained with the fusion with those resulting from the best single modality, the average improvement was of $4 \pm 3\%$. Noteworthy, this value was of $15 \pm 17\%$ when we compared the fusion with EEG, the modality that is the most used during BCI experiments.^{67,68}

Interestingly, the contribution of the different modalities to the fusion's performance was highly variable across subjects, as illustrated by the weights associated to the parameter λ_i (see Figure 5).

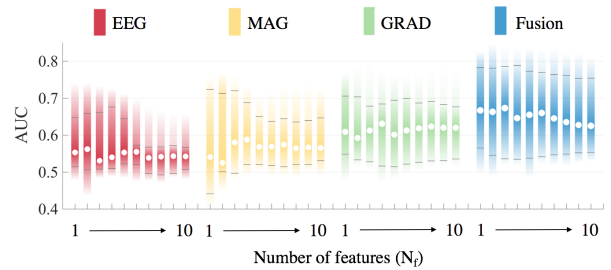


Figure 4. AUC distributions across the 15 subjects, for different modalities (EEG, MAG, GRAD, Fusion) and for different number of features N_f in the alpha band. White circles represent the associated median values.

Table 1. Individual performances overview across modalities. In bold, the best AUC obtained for a given subject.

	S01	S02	S03	S04	S05	S06	S07	S08	S09	S10	S11	S12	S13	S14	S15
<i>Band</i>	<i>alpha</i>	<i>alpha</i>	<i>beta</i>	<i>alpha</i>	<i>alpha</i>	<i>alpha</i>	<i>beta</i>	<i>beta</i>	<i>alpha</i>	<i>alpha</i>	<i>alpha</i>	<i>alpha</i>	<i>beta</i>	<i>alpha</i>	<i>beta</i>
EEG	0.53	0.55	0.48	0.56	0.57	0.55	0.57	0.50	0.60	0.66	0.53	0.55	0.70	0.73	0.60
MAG	0.47	0.48	0.53	0.51	0.50	0.55	0.52	0.62	0.57	0.58	0.69	0.76	0.59	0.64	0.71
GRAD	0.54	0.50	0.55	0.50	0.54	0.55	0.49	0.65	0.64	0.63	0.72	0.62	0.71	0.72	0.85
Fusion	0.55	0.55	0.56	0.57	0.58	0.59	0.57	0.67	0.66	0.70	0.80	0.77	0.76	0.79	0.85

4. Discussion

Improving performance remains one of the most challenging issues of non-invasive BCI systems.⁵⁵ High classification performance would allow effective control of the BCI and feedback to the subject that is crucial to establish an optimal interaction user-machine.^{19,67,68} BCI performance depends on several human and technological factors, including the ability of subjects to generate distinguishable brain features,³ as well as the robustness of signal processing and classification algorithms.⁵⁵

To this end, we recorded simultaneous EEG and MEG signals in a group of healthy subjects performing a motor imagery-based BCI task. Both EEG and MEG exhibit a high temporal resolution and the sensory motor-related changes are well known in the literature, as is their utility in standard BCI applications.^{19,44}

Notably, EEG and MEG signals are closely related but still they are respectively different in terms of sensitivity to radial and tangential currents, as well as to extracellular and intracellular currents.⁴⁰ These complementary properties could be simultaneously exploited by our fusion approach to better identify ERD mechanisms used here to control the BCI.

Results show that independently from the modality and the number of features, the best AUCs were obtained in alpha and (in a more limited way) beta bands, which is consistent with motor imagery's being associated with oscillations in the alpha and beta band.^{69,70} The proposed fusion approach showed that combining the most significant features in each modality led, in a large majority of subjects, to a reduction in the subjects' mental state misclassifications (see Table 1). By optimizing the choice of the features in each individual, we obtained an average classification improvement of 12.8 % as compared to separate EEG, MAG and GRAD clas-

sifiers (Table 1), suggesting a viable alternative to indirectly reduce the illiteracy phenomenon in non-invasive BCIs.^{71,72}

In this study, we also explored features from other frequency bands such as the gamma band (30-40 Hz). However, the obtained results gave marginal improvements as compared to alpha and beta bands. While gamma activity from intracranial recordings or local-field potentials is in general related to the initiation of motor/sensory function,^{25,73-77} the paucity of results in the gamma band could be here partly explained by the low signal-to-noise ratios and volume conduction effects that typically affect scalp EEG and MEG activity.⁷⁸⁻⁸⁰

The core of our approach consisted in weighting automatically the contribution of each modality in an effort to optimize performance. This is an important aspect as the discriminant power of features could suddenly change depending on many factors, such as impedance fluctuations or the presence of artifacts (e.g. isolated EEG electrode pops or MEG jumps). In this case, our fusion approach would take into account such transient fluctuations by silencing the affected modality through a lower weight λ_i in the classification. Slower changes could be related to the increasing ability of individuals to accurately control the BCI.^{55,67,81-83} In this case, our approach would progressively favor the spatio-temporal features of the modality that better capture those neural plasticity phenomena.

Interestingly, we noticed a high inter-subject variability in the attributed weights (Figure 5). While, this could be associated with the ability of each modality to detect different properties of the underlying ERD, further analysis, possibly in the source space,⁸⁴ is needed to elucidate this aspect and identify the neurophysiological correlates of such variability.

While the average AUC values were relatively low, we noticed that they are highly variable across

individuals (Table 1) and that they are close to those typically obtained in similar experiment settings.²⁷ Furthermore, it is important to mention that subjects were BCI-naïve and that no preprocessing was applied, with the goal of simulating real-life scenarios. Thus, while a proper pre-processing was likely.

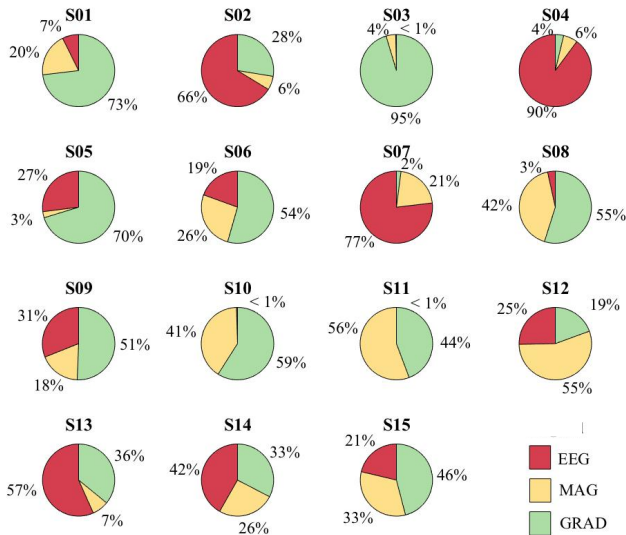


Figure 5. Contribution of different modalities to the individual performance. Pie-diagrams show the λ_i values (in percentage) obtained for each modality via the fusion approach.

to improve the accuracy in each single modality, our aim was rather to assess an improvement in the worst condition. Eventually, thirteen of our fifteen subjects presented a performance improvement with the classifier fusion.

Taken together, these results prove the potential advantage of using simultaneous E/MEG signals to enhance BCI performance. By using a rather simple classifier (LDA), we could include in the classification a reduced number of specific features involved in the motor-related neural mechanisms such as ERD in alpha and beta bands.

More sophisticated approaches using the whole feature space, such as support vector machines⁸⁵ and Riemannian geometry,⁸⁶ as well as alternative fusion strategies, such as boosting, voting, or stacking strategies,⁵⁵ but also classification in source space to improve spatial resolution^{42,87} and identification of

subject-specific time-frequency characteristics,⁸⁸ can be further evaluated to exploit their power in practical applications.

Finally, it is important to note that we tested our fusion approach offline by analyzing previously recorded data. To evaluate the feasibility in online applications, we estimated that for an epoch of 500 ms the time necessary to compute the features, perform the classification, and determine the parameter of the fusion, was approximately of 20 ms when $N_f = 5$. This value is actually compatible with current on-line settings using similar time windows and updating the feedback every 28 ms.⁴⁶

5. Conclusions

Our results showed that integrating information from simultaneous EEG and MEG signals improves BCI performance. E/MEG multimodal BCIs may turn out to be an effective approach to enhance the reliability of brain-machine interactions, but much of the progress will depend on the miniaturization of MEG scanners, which currently require a magnetic shielding room (MSR) and sensors cooled via a cryogenic system. Recent efforts proposing miniaturized and cryogenic-free MEG sensors^{43,89} and avoiding the use of MSRs⁹⁰ will hopefully offer practical solutions to increase MEG portability and boost the development of multimodal BCIs.

6. Acknowledgements

We would like to thank the anonymous reviewers for their constructive comments and suggestions. This work was partially supported by French program “Investissements d’avenir” ANR-10-IAIHU-06; “ANR-NIH CRCNS” ANR-15-NEUC-0006-02 and by Army Research Office (W911NF-14-1-0679). The funders had no role in study design, data collection and analysis, decision to publish, or preparation of the manuscript.

References

1. J. J. Vidal, Toward Direct Brain-Computer Communication, *Annual Review of Biophysics and Bioengineering* **2**(1) (1973) 157–180.
2. S. Bozinovski, M. Sestakov and L. Bozinovska, Using EEG alpha rhythm to control a mobile robot, *Proceedings of the Annual International Conference of the IEEE Engineering in Medicine and Biology Society*, November 1988, pp. 1515–1516 vol.3.

3. J. R. Wolpaw, N. Birbaumer, D. J. McFarland, G. Pfurtscheller and T. M. Vaughan, Braincomputer interfaces for communication and control, *Clinical Neurophysiology* **113** (June 2002) 767–791.
4. M. S. Fifer, G. Hotson, B. A. Wester, D. P. McMullen, Y. Wang, M. S. Johannes, K. D. Katyal, J. B. Helder, M. P. Para, R. J. Vogelstein, W. S. Anderson, N. V. Thakor and N. E. Crone, Simultaneous neural control of simple reaching and grasping with the modular prosthetic limb using intracranial EEG, *IEEE Trans Neural Syst Rehabil Eng* **22** (May 2014) 695–705.
5. T. Carlson and J. d. R. Millan, Brain-Controlled Wheelchairs: A Robotic Architecture, *IEEE Robotics Automation Magazine* **20** (March 2013) 65–73.
6. K. LaFleur, K. Cassady, A. Doud, K. Shades, E. Rogin and B. He, Quadcopter control in three-dimensional space using a noninvasive motor imagery-based brain-computer interface, *Journal of Neural Engineering* **10** (August 2013) p. 046003.
7. J. Jin, B. Z. Allison, T. Kaufmann, A. Kbler, Y. Zhang, X. Wang and A. Cichocki, The changing face of P300 BCIs: a comparison of stimulus changes in a P300 BCI involving faces, emotion, and movement, *PloS One* **7**(11) (2012) p. e49688.
8. H.-J. Hwang, J.-H. Lim, Y.-J. Jung, H. Choi, S. W. Lee and C.-H. Im, Development of an SSVEP-based BCI spelling system adopting a QWERTY-style LED keyboard, *Journal of Neuroscience Methods* **208** (June 2012) 59–65.
9. K. Kashiwara, A brain-computer interface for potential non-verbal facial communication based on EEG signals related to specific emotions, *Frontiers in Neuroscience* **8** (2014) p. 244.
10. L. Naci, R. Cusack, V. Z. Jia and A. M. Owen, The brain's silent messenger: using selective attention to decode human thought for brain-based communication, *J. Neurosci.* **33** (May 2013) 9385–9393.
11. A. Ortiz-Rosario and H. Adeli, Brain-computer interface technologies: from signal to action, *Rev Neurosci* **24**(5) (2013) 537–552.
12. J. J. Daly and J. R. Wolpaw, Braincomputer interfaces in neurological rehabilitation, *The Lancet Neurology* **7** (November 2008) 1032–1043.
13. G. Prasad, P. Herman, D. Coyle, S. McDonough and J. Crosbie, Applying a brain-computer interface to support motor imagery practice in people with stroke for upper limb recovery: a feasibility study, *Journal of Neuroengineering and Rehabilitation* **7** (December 2010) p. 60.
14. C. E. King, P. T. Wang, L. A. Chui, A. H. Do and Z. Nenadic, Operation of a brain-computer interface walking simulator for individuals with spinal cord injury, *Journal of Neuroengineering and Rehabilitation* **10** (July 2013) p. 77.
15. C. Chatelle, S. Chennu, Q. Noirhomme, D. Cruse, A. M. Owen and S. Laureys, Brain-computer interfacing in disorders of consciousness, *Brain Injury* **26**(12) (2012) 1510–1522.
16. S. Kim and N. Birbaumer, Real-time functional MRI neurofeedback: a tool for psychiatry, *Current Opinion in Psychiatry* **27** (September 2014) 332–336.
17. A. Burns, H. Adeli and J. A. Buford, Brain-computer interface after nervous system injury, *Neuroscientist* **20** (December 2014) 639–651.
18. C. Guger, B. Allison and J. Ushiba, *Brain-Computer Interface Research*, springer science & business media edn. (Springer Science & Business Media, 2013).
19. C. Vidaurre and B. Blankertz, Towards a Cure for BCI Illiteracy, *Brain Topography* **23**(2) (2010) 194–198.
20. B. Z. Allison and C. Neuper, Could Anyone Use a BCI?, *Brain-Computer Interfaces*, eds. D. S. Tan and A. Nijholt, *Human-Computer Interaction Series* (Springer London, 2010), pp. 35–54.
21. C. Zickler, V. Di Donna, V. Kaiser, A. Al-Khodairy, S. Kleih, A. Kbler, M. Malavasi, D. Mattia, S. Mongardi, C. Neuper, M. Rohm, R. Rupp, P. Staiger-Slzer and E. J. Hoogerwerf, BCI applications for people with disabilities: Defining user needs and user requirements, *Assistive Technology Research Series, Assistive Technology Research Series* **25** 2009, pp. 185–189.
22. J. Toppi, M. Riseti, L. R. Quitadamo, M. Petti, L. Bianchi, S. Salinari, F. Babiloni, F. Cincotti, D. Mattia and L. Astolfi, Investigating the effects of a sensorimotor rhythm-based BCI training on the cortical activity elicited by mental imagery, *Journal of Neural Engineering* **11** (June 2014) p. 035010.
23. V. Kaiser, G. Bauernfeind, A. Kreiling, T. Kaufmann, A. Kbler, C. Neuper and G. R. Müller-Putz, Cortical effects of user training in a motor imagery based brain-computer interface measured by fNIRS and EEG, *NeuroImage* **85 Pt 1** (January 2014) 432–444.
24. S. Perdakis, R. Leeb and J. d. R. Milln, Subject-oriented training for motor imagery brain-computer interfaces, *Conf Proc IEEE Eng Med Biol Soc* **2014** (2014) 1259–1262.
25. J. D. Wander, T. Blakely, K. J. Miller, K. E. Weaver, L. A. Johnson, J. D. Olson, E. E. Fetz, R. P. N. Rao and J. G. Ojemann, Distributed cortical adaptation during learning of a braincomputer interface task, *Proceedings of the National Academy of Sciences of the United States of America* **110** (June 2013) 10818–10823.
26. C. Vidaurre, C. Sannelli, K. R. Müller and B. Blankertz, Co-adaptive calibration to improve BCI efficiency, *Journal of Neural Engineering* **8** (April 2011) p. 025009.
27. G. Pfurtscheller, B. Z. Allison, C. Brunner, G. Bauernfeind, T. Solis-Escalante, R. Scherer, T. O. Zander, G. Mueller-Putz, C. Neuper and N. Birbaumer, The hybrid BCI, *Frontiers in Neuroscience* **4** (2010) p. 30.
28. F. Pichiorri, F. D. V. Fallani, F. Cincotti, F. Ba-

- biloni, M. Molinari, S. C. Kleih, C. Neuper, A. Kbler and D. Mattia, Sensorimotor rhythm-based brain-computer interface training: the impact on motor cortical responsiveness, *Journal of Neural Engineering* **8**(2) (2011) p. 025020.
29. F. Pichiorri, G. Morone, M. Petti, J. Toppi, I. Pisotta, M. Molinari, S. Paolucci, M. Inghilieri, L. Astolfi, F. Cincotti and D. Mattia, Brain-computer interface boosts motor imagery practice during stroke recovery, *Annals of Neurology* **77** (May 2015) 851–865.
 30. G. Mller-Putz, R. Leeb, M. Tangermann, J. Hhne, A. Kbler, F. Cincotti, D. Mattia, R. Rupp, K. R. Mller and J. d. R. Milln, Towards Noninvasive Hybrid Brain-Computer Interfaces: Framework, Practice, Clinical Application and Beyond, *Proceedings of the IEEE* **103**(6) (2015) 926–943.
 31. R. Sitaram, A. Caria and N. Birbaumer, Hemodynamic braincomputer interfaces for communication and rehabilitation, *Neural Networks* **22** (November 2009) 1320–1328.
 32. S. Fazli, J. Mehnert, J. Steinbrink, G. Curio, A. Villringer, K. Mller and B. Blankertz, Enhanced performance by a hybrid NIRSEEG brain computer interface, *NeuroImage* **59** (January 2012) 519–529.
 33. Y. Tomita, F.-B. Vialatte, G. Dreyfus, Y. Mitsukura, H. Bakardjian and A. Cichocki, Bimodal BCI using simultaneously NIRS and EEG, *IEEE transactions on bio-medical engineering* **61** (April 2014) 1274–1284.
 34. A. P. Buccino, H. O. Keles and A. Omurtag, Hybrid EEG-fNIRS Asynchronous Brain-Computer Interface for Multiple Motor Tasks, *PloS One* **11**(1) (2016) p. e0146610.
 35. L. Perronnet, A. Lcuyer, M. Mano, E. Bannier, F. Lotte, M. Clerc and C. Barillot, Unimodal Versus Bimodal EEG-fMRI Neurofeedback of a Motor Imagery Task, *Frontiers in Human Neuroscience* **11** (2017).
 36. B. N. Cuffin and D. Cohen, Comparison of the magnetoencephalogram and electroencephalogram, *Electroencephalography and Clinical Neurophysiology* **47** (August 1979) 132–146.
 37. C. D. Geisler and G. L. Gerstein, The surface EEG in relation to its sources, *Electroencephalography and Clinical Neurophysiology* **13** (December 1961) 927–934.
 38. M. R. Delucchi, B. Garoutte and R. B. Aird, The scalp as an electroencephalographic averager, *Electroencephalography and Clinical Neurophysiology* **14** (April 1962) 191–196.
 39. R. Cooper, A. L. Winter, H. J. Crow and W. G. Walter, Comparison of subcortical, cortical and scalp activity using chronically indwelling electrodes in man, *Electroencephalography and Clinical Neurophysiology* **18** (February 1965) 217–228.
 40. M. Hmlinen, R. Hari, R. J. Ilmoniemi, J. Knuutila and O. V. Lounasmaa, Magnetoencephalography-theory, instrumentation, and applications to noninvasive studies of the working human brain, *Reviews of Modern Physics* **65** (April 1993) 413–497.
 41. C. C. Wood, D. Cohen, B. N. Cuffin, M. Yarita and T. Allison, Electrical sources in human somatosensory cortex: identification by combined magnetic and potential recordings, *Science (New York, N.Y.)* **227** (March 1985) 1051–1053.
 42. D. Sharon, M. S. Hmlinen, R. B. H. Tootell, E. Halgren and J. W. Belliveau, The advantage of combining MEG and EEG: Comparison to fMRI in focally stimulated visual cortex, *NeuroImage* **36** (July 2007) 1225–1235.
 43. E. Boto, S. S. Meyer, V. Shah, O. Alem, S. Knappe, P. Kruger, T. M. Fromhold, M. Lim, P. M. Glover, P. G. Morris, R. Bowtell, G. R. Barnes and M. J. Brookes, A new generation of magnetoencephalography: Room temperature measurements using optically-pumped magnetometers, *NeuroImage* **149**(Supplement C) (2017) 404 – 414.
 44. J. Mellinger, G. Schalk, C. Braun, H. Preissl, W. Rosenstiel, N. Birbaumer and A. Kbler, An MEG-based brain-computer interface (BCI), *NeuroImage* **36**(3) (2007) 581–593.
 45. H.-L. Halme and L. Parkkonen, Comparing Features for Classification of MEG Responses to Motor Imagery, *PLOS ONE* **11** (December 2016) p. e0168766.
 46. G. Schalk, D. J. McFarland, T. Hinterberger, N. Birbaumer and J. R. Wolpaw, BCI2000: a general-purpose brain-computer interface (BCI) system, *IEEE transactions on bio-medical engineering* **51** (June 2004) 1034–1043.
 47. R. Oostenveld, P. Fries, E. Maris and J.-M. Schoffelen, FieldTrip: Open Source Software for Advanced Analysis of MEG, EEG, and Invasive Electrophysiological Data, FieldTrip: Open Source Software for Advanced Analysis of MEG, EEG, and Invasive Electrophysiological Data, *Computational Intelligence and Neuroscience, Computational Intelligence and Neuroscience* **2011**, **2011** (December 2010) p. e156869.
 48. J. R. Wolpaw, D. J. McFarland, T. M. Vaughan and G. Schalk, The Wadsworth Center brain-computer interface (BCI) research and development program, *IEEE transactions on neural systems and rehabilitation engineering: a publication of the IEEE Engineering in Medicine and Biology Society* **11** (June 2003) 204–207.
 49. P. C. Hansen, M. L. Kringelbach and R. Salmelin, *MEG: An introduction to Methods*, oxford university press edn. 2010.
 50. S. Taulu and J. Simola, Spatiotemporal signal space separation method for rejecting nearby interference in MEG measurements, *Phys Med Biol* **51** (April 2006) 1759–1768.
 51. D. Slepian, Prolate spheroidal wave functions, fourier analysis, and uncertainty #x2014; V: the discrete case, *The Bell System Technical Journal* **57**

- (May 1978) 1371–1430.
52. S. Bozinovski, Controlling Robots Using EEG Signals, Since 1988, *ICT Innovations 2012, Advances in Intelligent Systems and Computing* (Springer, Berlin, Heidelberg, 2013), pp. 1–11.
 53. K. Fukunaga, *Introduction to Statistical Pattern Recognition (2Nd Ed.)* (Academic Press Professional, Inc., San Diego, CA, USA, 1990).
 54. R. O. Duda, P. E. Hart and D. G. Stork, *Pattern Classification (2Nd Edition)* (Wiley-Interscience, 2000).
 55. F. Lotte, M. Congedo, A. Lcuyer, F. Lamarche and B. Arnaldi, A review of classification algorithms for EEG-based brain-computer interfaces, *Journal of Neural Engineering* **4** (June 2007) R1–R13.
 56. D. Ruta and B. Gabrys, An Overview of Classifier Fusion Methods, *Computing and Information Systems* **7** (February 2000) 1–10.
 57. F. Roli and G. Fumera, Analysis of Linear and Order Statistics Combiners for Fusion of Imbalanced Classifiers, *Multiple Classifier Systems, Lecture Notes in Computer Science*, (Springer, Berlin, Heidelberg, June 2002), pp. 252–261.
 58. F. Roli, Multiple Classifier Systems, *Encyclopedia of Biometrics*, eds. S. Z. Li and A. Jain (Springer US, 2009), pp. 981–986.
 59. I. Witten, E. Frank, M. Hall and C. Pal, *Data Mining - 4th Edition*, morgan kaufmann edn., (2016).
 60. J. Zar, *Biostatistical analysis*, pearson education edn. 1999.
 61. A. Delorme and S. Makeig, EEGLAB: an open source toolbox for analysis of single-trial EEG dynamics including independent component analysis, *J. Neurosci. Methods* **134** (March 2004) 9–21.
 62. G. Pfurtscheller and F. H. Lopes da Silva, Event-related EEG/MEG synchronization and desynchronization: basic principles, *Clinical Neurophysiology* **110** (November 1999) 1842–1857.
 63. F. Tadel, S. Baillet, J. Mosher, D. Pantazis and R. Leahy, Brainstorm: A User-Friendly Application for MEG/EEG Analysis, *Computational Intelligence and Neuroscience* **2011** (January 2011).
 64. C. Neuper and G. Pfurtscheller, Event-related dynamics of cortical rhythms: frequency-specific features and functional correlates, *Int J Psychophysiol* **43** (December 2001) 41–58.
 65. C. Neuper, R. Scherer, M. Reiner and G. Pfurtscheller, Imagery of motor actions: Differential effects of kinesthetic and visuomotor mode of imagery in single-trial EEG, *Cognitive Brain Research* **25** (December 2005) 668–677.
 66. G. Pfurtscheller, C. Brunner, A. Schlgl and F. H. Lopes da Silva, Mu rhythm (de)synchronization and EEG single-trial classification of different motor imagery tasks, *NeuroImage* **31** (May 2006) 153–159.
 67. M. Clerc, L. Bougrain and F. Lotte, *Brain-Computer Interfaces 1: Methods and Perspectives*, wiley edn. (Wiley, 2016).
 68. M. Clerc, L. Bougrain and F. Lotte, *Brain-Computer Interfaces 2: Technology and Applications*, wiley edn. (Wiley, 2016).
 69. G. Pfurtscheller, C. Neuper, D. Flotzinger and M. Pregenzer, EEG-based discrimination between imagination of right and left hand movement, *Electroencephalogr Clin Neurophysiol* **103** (December 1997) 642–651.
 70. G. Pfurtscheller and C. Neuper, Motor imagery and direct brain-computer communication, *Proceedings of the IEEE* **89** (July 2001) 1123–1134.
 71. D. J. McFarland and J. R. Wolpaw, Brain-Computer Interfaces for Communication and Control, *Communications of the ACM* **54**(5) (2011) 60–66.
 72. J. v. Erp, F. Lotte and M. Tangermann, Brain-Computer Interfaces: Beyond Medical Applications, *Computer* **45** (April 2012) 26–34.
 73. C. Tallon-Baudry and O. Bertrand, Oscillatory gamma activity in humans and its role in object representation, *Trends in Cognitive Sciences* **3** (April 1999) 151–162.
 74. E. Rodriguez, N. George, J.-P. Lachaux, J. Martinerie, B. Renault and F. J. Varela, Perception's shadow: long-distance synchronization of human brain activity, *Nature* **397** (February 1999) p. 430.
 75. R. T. Canolty, E. Edwards, S. S. Dalal, M. Soltani, S. S. Nagarajan, H. E. Kirsch, M. S. Berger, N. M. Barbaro and R. T. Knight, High Gamma Power Is Phase-Locked to Theta Oscillations in Human Neocortex, *Science* **313** (September 2006) 1626–1628.
 76. D. Cheyne, S. Bells, P. Ferrari, W. Gaetz and A. C. Bostan, Self-paced movements induce high-frequency gamma oscillations in primary motor cortex, *NeuroImage* **42** (August 2008) 332–342.
 77. S. D. Muthukumaraswamy, Functional Properties of Human Primary Motor Cortex Gamma Oscillations, *Journal of Neurophysiology* **104** (September 2010) 2873–2885.
 78. M. Grosse-Wentrup, B. Schlopf and J. Hill, Causal influence of gamma oscillations on the sensorimotor rhythm, *NeuroImage* **56** (May 2011) 837–842.
 79. M. Grosse-Wentrup and B. Schlopf, High -power predicts performance in sensorimotor-rhythm brain-computer interfaces, *J Neural Eng* **9** (August 2012) p. 046001.
 80. C. Jeunet, B. N'Kaoua, S. Subramanian, M. Hachet and F. Lotte, Predicting Mental Imagery-Based BCI Performance from Personality, Cognitive Profile and Neurophysiological Patterns, *PLoS ONE* **10**(12) (2015) p. e0143962.
 81. E. A. Curran and M. J. Stokes, Learning to control brain activity: A review of the production and control of EEG components for driving brain-computer interface (BCI) systems, *Brain and Cognition* **51** (April 2003) 326–336.
 82. B. H. Dobkin, Braincomputer interface technology as a tool to augment plasticity and outcomes for neurological rehabilitation, *The Journal of Physiology* **579**

- (March 2007) 637–642.
83. M. Grosse-Wentrup, D. Mattia and K. Oweiss, Using braincomputer interfaces to induce neural plasticity and restore function, *J. Neural Eng.* **8**(2) (2011) p. 025004.
 84. J. Gross, S. Baillet, G. R. Barnes, R. N. Henson, A. Hillebrand, O. Jensen, K. Jerbi, V. Litvak, B. Maess, R. Oostenveld, L. Parkkonen, J. R. Taylor, V. van Wassenhove, M. Wibral and J.-M. Schoffelen, Good practice for conducting and reporting MEG research, *Neuroimage* **65** (January 2013) 349–363.
 85. T. Lai, M. Schrder, T. Hinterberger, J. Weston, M. Bogdan, N. Birbaumer and B. Schalkopf, Support vector channel selection in BCI, *IEEE Transactions on Biomedical Engineering* **51**(6) (2004) 1003–10.
 86. A. Barachant, S. Bonnet, M. Congedo and C. Jutten, Classification of covariance matrices using a Riemannian-based kernel for BCI applications, *Neurocomputing* **112** (July 2013) 172–178.
 87. M. Muthuraman, H. Hellriegel, N. Hoogenboom, A. R. Anwar, K. G. Mideksa, H. Krause, A. Schnitzler, G. Deuschl and J. Raethjen, Beamformer source analysis and connectivity on concurrent EEG and MEG data during voluntary movements, *PloS One* **9**(3) (2014).
 88. Y. Yang, S. Chevallier, J. Wiart and I. Bloch, Time-frequency optimization for discrimination between imagination of right and left hand movements based on two bipolar electroencephalography channels, *EURASIP Journal on Advances in Signal Processing* **2014**(1) (2014) p. 38.
 89. R. Jimnez-Martnez and S. Knappe, Microfabricated Optically-Pumped Magnetometers, *High Sensitivity Magnetometers, Smart Sensors, Measurement and Instrumentation* (Springer, Cham, 2017), pp. 523–551.
 90. A. R. Sorbo, G. Lombardi, L. La Brocca, G. Guida, R. Fenici and D. Brisinda, Unshielded magnetocardiography: Repeatability and reproducibility of automatically estimated ventricular repolarization parameters in 204 healthy subjects, *Ann Noninvasive Electrocardiol* (December 2017).

Appendix A

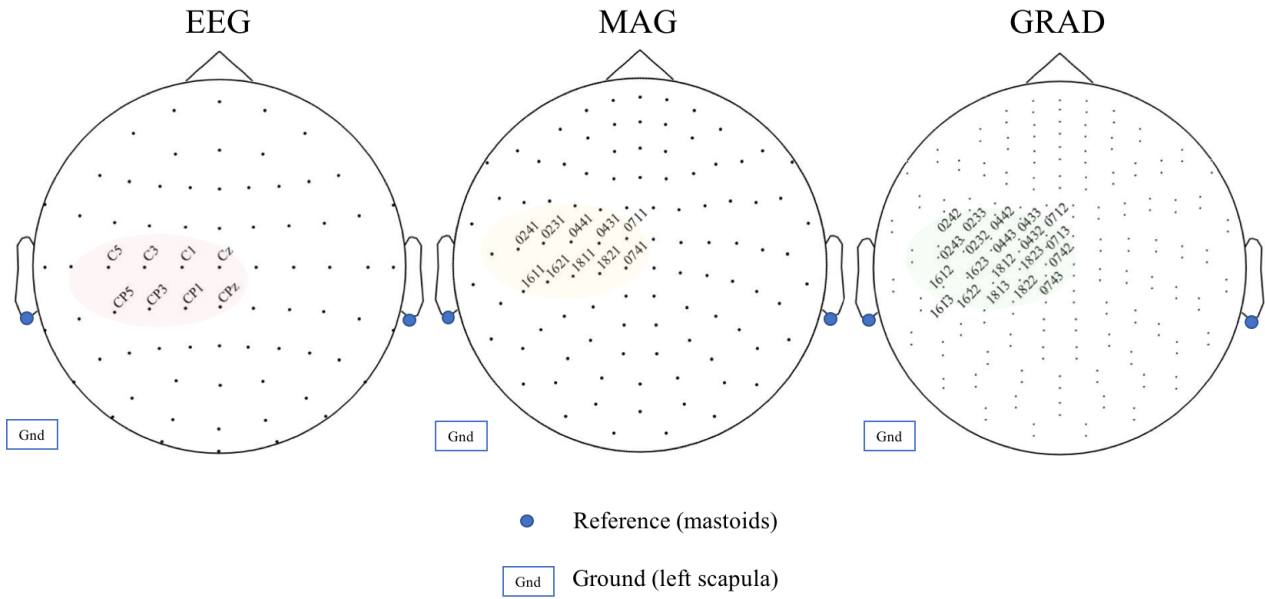


Figure A.1. Pre-selected EEG and MEG sensors (left motor area).